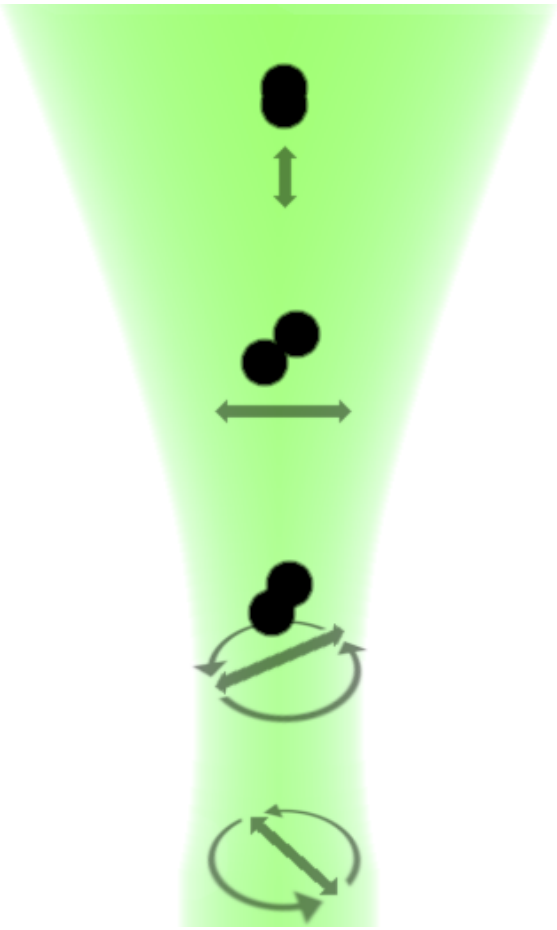

Dynamics of Optically Levitated Microdumbbells

Bachelor's thesis in Physics

LUDVIG LINDAHL
SIXTEN FURENÄS
TOBIAS HAINER

DEPARTMENT OF PHYSICS

UNIVERSITY OF GOTHENBURG
CHALMERS UNIVERSITY OF TECHNOLOGY
www.chalmers.se
Gothenburg, Sweden 2021

BACHELORS'S THESIS IN PHYSICS

Dynamics of Optically Levitated Microdumbbells

LUDVIG LINDAHL
SIXTEN FURENÄS
TOBIAS HAINER

UNIVERSITY OF
GOTHENBURG

CHALMERS
UNIVERSITY OF TECHNOLOGY

Department of Physics
Research group for Laser Spectroscopy
University of Gothenburg
Chalmers University of Technology
Gothenburg, Sweden 2021

Dynamics of Optically Levitated Microdumbbells
LUDVIG LINDAHL
SIXTEN FURENÄS
TOBIAS HAINER

Supervisor: Javier Tello Marmolejo, GU Department of Physics
Examiner: Jan Swenson, Chalmers Department of Physics
Examiner: Martina Ahlberg, GU Department of Physics

Bachelors's Thesis TIFX04-21-23
Department of Physics
Research group for Laser Spectroscopy
University of Gothenburg
Chalmers University of Technology

Cover: An illustration of a dumbbell under the influence of polarized light in different vertical regimes. Typeset in LaTeX
Gothenburg, Sweden 2021

Acknowledgements

First, we would like to thank Javier Tello Marmolejo for being a great teacher and guide when introducing us to the world of optical levitation. This thesis would not have been possible without his support.

We would like to thank Dag Hanstorp for the warm welcome into his research group and all the great Thursday meetings.

We would like to thank Oscar Isaksson for sharing and helping us with his experimental set up.

Also, we would like to thank Pablo Hernandez Munguia for being great to talk with when we ran into issues in the lab.

Abstract

As light carries momentum, enough force can be applied to small particles from a vertical pointing laser to counteract the gravitational force it feels, thus levitating it in thin air. Oblong nanoparticles under these conditions have shown themselves to align their long axis with the laser's polarization and rotate with it. The precise torque control and measurements these levitated objects offer are hypothesised to pave way for future quantum development. Previous experiments have also created the fastest man made rotor at 1 GHz, which was achieved by a levitated nanodumbbell in circularly polarized light. However, the behavior of these levitated oblong objects with regards to polarization is not as well known at bigger scales. Here we have studied how polarization affects micrometric dumbbells. We found a direct connection between the dumbbells' elevation in the trap and their reaction to the polarization, giving rise to different regimes. Furthermore, under circularly polarized light we showed a cyclical process where a dumbbell would start to oscillate and rise in elevation in the trap. At a certain point, this oscillation would fade and the particle would fall down in the trap and repeat the same steps. Our results show a clear difference between dumbbells at nanoscale compared to microscale, with models presented to explain the different behaviors. Many of the phenomena that we have observed may serve as a subject of future research. These phenomena include dumbbell turnovers, exploring the dumbbell's alignment in the stationary regime and finding a theoretical explanation for the different regimes of dumbbell-polarization interaction.

Contents

1 Introduction

Since Arthur Ashkin first reported the use of focused laser beams to optically trap microscopic particles[1], his findings have proven themselves to be of great importance in fields such as biology, nanotechnology and quantum optics. The principle of his discovery relies on the fact that light carries a small amount of momentum and when absorbed, reflected, or refracted by an object, will transfer momentum to it. Absorption and reflection push the particle along the path of the laser, creating a scattering force in that direction. Refraction instead pushes it in the direction of greatest laser intensity, which creates a gradient force. Ashkin successfully demonstrated that momentum from a laser could, when focused correctly, produce a force larger than the gravitational force on a microscopic particle in the lasers path, hence trapping the particle in thin air.

At nanoscales, oblong levitated objects have previously been studied and their behavior mapped out. J. Bang *et al.* report cooling levitated nanodumbbells in linear polarization, and having them align with it [2]. J. Ahn *et al.* have shown that levitated dumbbells offer precise torque control [3]. They also drive a nanodumbbell to rotate at 1 GHz under circularly polarized light, which is the fastest man made rotor to date. S. Kuhn *et al.* have trapped nanorods and show great control of these, which may have future use in fields such as optomechanics [4]. So overall, these oblong rods, dumbbells, and ellipsoids provide an unprecedented method of precise torque control and detection. They may play a big part in future quantum development, as they are hypothesised to be useful in experiments regarding the electron spin and the Casimir effect.

The behavior of levitated oblong objects beyond the nanoscale is less known, with little research regarding how these particles react to pressure change, polarization and so on.

The aim of this thesis is to map out how microscale oblong objects, especially dumbbells, react to different polarization and find a way to intuitively describe this behavior with a model. A method for producing dumbbells was developed and used to create and study dumbbells under both linear and circular polarization. The results gave rise to different vertical regimes where the dumbbells reaction to the polarization varied. Also, a cyclical process was found for dumbbells trapped in circularly polarized light, which is explained with the regimes.

2 Theory

2.1 Optical Levitation

In an optical trap, the interaction of the laser beam and the trapped object gives rise to two forces acting on the object, both originating from radiation pressure. The scattering force works in the direction of the laser beam while the gradient force has the direction of the gradient of the beam, pushing the trapped object towards the region of maximum intensity. In a levitation trap the scattering force balances out the gravitational force as illustrated in figure 1. [5]

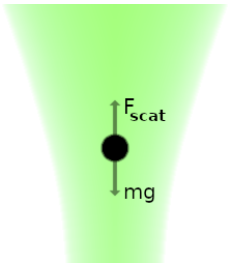

Figure 1: The scattering force, produced through radiation pressure, pushes the trapped particle upwards, counteracting gravity.

Depending on the size of the particle in relation to the wavelength of the laser, different approximations can be employed. When the size of the object is much larger than the wavelength, the propagation of the beam and interaction with the object can be described in terms of ray optics. This is known as the geometric regime. [6]

A momentum can be associated with each incident ray of light where the magnitude of this momentum correlates with the intensity of the light. Through refraction and reflection, these rays change direction and hence momentum. By Newtons third law, a force acting on the trapped object can be expressed in terms of the change of momentum for each ray. Summing over all incident rays, the total force can be calculated.

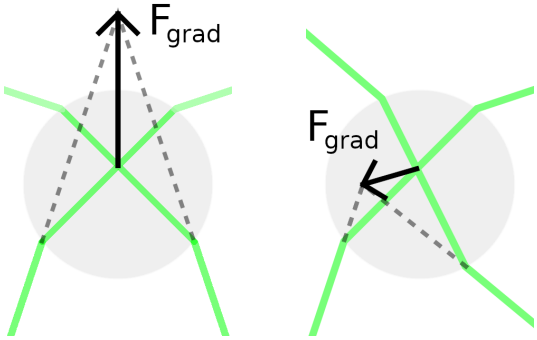

Figure 2: Refraction of light causes a change of momentum resulting in a force, directed towards the focal point of the beam. In these examples, the gradient force pushes the trapped particle upwards and sideways.

The momentum of a single photon is given by,

$$p = \frac{h}{\lambda}, \tag{1}$$

where h is planck's constant and λ is the wavelength. The energy of a single photon is given by,

$$E_{\text{photon}} = \frac{n_1 hc}{\lambda} = n_1 pc, \tag{2}$$

where c is the speed of light and n_1 is the refractive index. Differentiating both sides with respect to time and multiplying by the number of photons in a ray leads to,

$$P = n_1 \frac{\mathrm{d}p}{\mathrm{d}t} c, \tag{3}$$

where P is the power of a ray and $\frac{\mathrm{d}p}{\mathrm{d}t}$ is the momentum per second associated with the ray.

The refraction and reflection of light can be described with the familiar Snell's law,

$$n_1 \sin\theta_1 = n_2 \sin\theta_2 \tag{4}$$

and Fresnel equations,

$$r_\mathrm{s} = \frac{n_1 \cos\theta_i - n_2 \cos\theta_t}{n_1 \cos\theta_i + n_2 \cos\theta_t}, \tag{5}$$

$$t_\mathrm{s} = \frac{2n_1 \cos\theta_i}{n_1 \cos\theta_i + n_2 \cos\theta_t}, \tag{6}$$

$$r_\mathrm{p} = \frac{n_2 \cos\theta_i - n_1 \cos\theta_t}{n_2 \cos\theta_i + n_1 \cos\theta_t}, \tag{7}$$

$$t_\mathrm{p} = \frac{2n_1 \cos\theta_i}{n_2 \cos\theta_i + n_1 \cos\theta_t}, \tag{8}$$

where t is a transmission coefficient and r is a reflection coefficient. The subscript p signifies polarization parallel to the surface and s signifies polarization perpendicular to the surface. By applying these laws on each ray, the change of momentum experienced by a ray during a period of time can be inferred. This is equivalent to a force acting on the trapped object.

The scattering force can be written as,

$$F_\mathrm{scat} = Q_\mathrm{scat} \frac{n_1 P}{c}, \tag{9}$$

where Q_scat can be calculated by integrating over all rays, taking the intensity distribution into consideration [7].

The value of the Q_s-coefficient is always somewhere in the range from 0 to 2. It can be interpreted as a measure of transparency, absorbtion and reflection for the different rays of the laser beam when hitting the trapped particle. If the object were fully transparent, no refraction and hence change of momentum would occur leading to $Q = 0$. If all light were absorbed, the momentum of incident rays would be nullified, leading to $Q = 1$. Lastly, if all rays were reflected, the change of momentum would be two times the initial momentum, leading to $Q = 2$.

The explanation for the gradient force can be found in the intensity distribution and ray direction of the laser. It can be seen in the right part of figure 2 that a particle displaced to the right will feel a restoring force as a result of the changed ray directions. Additionally, for a Gaussian beam, the intensity reaches a maximum value in the middle, and decays exponentially to zero further away. In such a situation, it can be seen in figure 2 that the ray which enters from the left would have a higher intensity than the ray from the right. When the former ray exits it has gained momentum to the right, and the latter has gained momentum to the left. For the conservation of momentum, the particle must thus have gained an equal momentum in the opposite directions. As the left ray is more intense, and thus carries greater momentum, the particle will feel an additional net force to the left.

2.2 Gaussian Beam

A Gaussian beam focused by a lens converges towards the focal point but, because of the diffraction limit, it does not become singular, instead converging to a minimal beam cross-section [8]. An illustration can be seen in figure 3. The minimal beam radius is called the beam waist, ω_0.

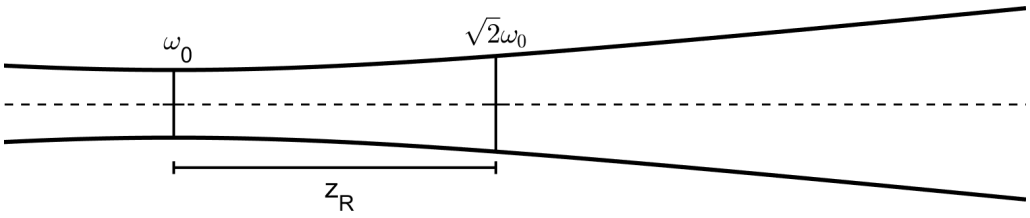

Figure 3: An illustration of a Gaussian beam with its beam waist and Rayleigh length marked.

The widening of the beam radius can be described by the formula

$$\omega(z) = \omega_0 \left[1 + \left(\frac{\lambda z}{\pi \omega_0^2}\right)^2\right]^{1/2}, \tag{10}$$

where λ is the wavelength of the beam, z is the distance from the beam waist and ω_0 is the beam waist. From this formula, the so called Rayleigh length, referring to the distance over which the beam widens by a factor of $\sqrt{2}$, can be derived, giving,

$$z_{\mathrm{R}} = \frac{\pi \omega_0^2}{\lambda}. \tag{11}$$

To approximately calculate the beam waist of a focused beam, the following equation can be used,

$$\omega_0 = 2\frac{\lambda f}{\pi D}, \tag{12}$$

where f is the focal length and D is the aperture diameter, in this case the diameter of the beam before the lens. By multiplying the above equation by two, the beam waist diameter, $2\omega_0$ is calculated instead of the radius.

2.3 Single Particle Potential

The movement of a single particle can be described using the equations for a damped, driven, harmonic oscillator. As a first approximation, a particle displaced from the point of stability in the trap will feel a restoring force which is proportional to the displacement,

$$F_{\mathrm{r}} = -kx, \tag{13}$$

where k is the trap stiffness, and x is the displacement from the point of stability. For sufficiently large displacements, neither the gradient force nor the restoring vertical force will increase linearly. Nevertheless, for small displacements in the laser, this approximation is valid.

To account for the drag from the air, a damping force can be used to modify the harmonic oscillator. According to Stokes' law, this force of friction will be

$$F_{\mathrm{f}} = -6\pi\eta r v, \tag{14}$$

where η is the viscosity of air, r is the radius of the particle, and $v = \mathrm{d}x/\mathrm{d}t$ is the velocity of the particle. Finally, for completeness, an as of yet undetermined driving force F_{d} can be applied. This gives

$$F_{\mathrm{tot}} = F_{\mathrm{r}} + F_{\mathrm{f}} + F_{\mathrm{d}} = ma, \tag{15}$$

where m is the mass of the particle and $a = \mathrm{d}^2x/\mathrm{d}t^2$ is the acceleration of the particle. Thus, the equation of motion becomes

$$\frac{\mathrm{d}^2x}{\mathrm{d}t^2} + \alpha\frac{\mathrm{d}x}{\mathrm{d}t} + \beta^2 x = \frac{F_{\mathrm{d}}}{m}, \tag{16}$$

where $\alpha = 6\pi\eta r/m$, and $\beta^2 = k/m$. β is the angular frequency which would be achieved for a harmonic oscillator in the absence of driving and damping forces.

Two significant results can be found with this equation. Firstly, in the absence of a driving force, any solution will eventually decay towards zero, as a result of the damping. Secondly, if the driving force is sinusoidal, the solution will eventually oscillate with the same frequency as the driving force [6].

2.4 Brownian motion of trapped particles

The surrounding air molecules can influence trapped particles in two ways. Firstly, the air resistance acts as a dampening force, stabilising particles in motion. Secondly, air molecules colliding with the trapped particle give rise to a random motion known as Brownian motion.

The Brownian motion can be a useful tool for empirically calculating the trap stiffness k in an environment where the damping force is not negligible. In such an environment, it is impossible to calculate k by directly measuring the oscillating motion of the particle, as this motion quickly decays to zero. Instead, the random Brownian motion of the particle can be used, as this motion spontaneously puts the particle at higher points of the potential. The higher the point, the less likely the particle is to gain enough energy to reach it. The random displacements of the particle over time represent a probability distribution. Through Boltzmann statistics the particle's trapping potential can be measured. Naturally, by knowing this potential, a value for k can be calculated [9].

2.5 Polarisation Alignment

Using the electric dipole approximation, the polarizability of small oblong objects, such as ellipsoids, rods and dumbbells, is the largest along its longer axis. Therefore, the electric field from the laser polarization applies a restoring force on these objects aligning their long side with it [3].

At low pressure, when the Brownian force is smaller than the polarization's restoring force, a nanoscale dielectric oblong object in a linearly polarized beam will stabilize and align with the electric field[4]. If the same situation takes place under circular polarization, the driving force applied to the object is constantly changing direction leading to a change in direction of stability. This motion is best described as a damped driven oscillator, the damping is linearly proportional to the environment's viscosity.

At larger scales, another effect may take place, as the amount of light reflected or transmitted when encountering a surface depends on the polarization, as described by the Fresnel equations. Specifically, light which is polarized parallel to the surface will be reflected more than light polarized perpendicularly to that direction. This means that, although the net force from parallel sides is still 0, the force from the scattered light on a trapped particle will be different for perpendicular sides. On the sides of the particle which are parallel to the polarization of the light, the force will be weaker, because of the greater reflection. On the other, perpendicular sides, the force will instead be stronger. This means that the gradient force will be stronger for a particle which is displaced from the stability point in a direction parallel to the polarization, as compared to a displacement perpendicular to the polarization.

3 Method

3.1 Experimental Setup

A 532 nm CW linearly polarized laser (Laser Quantum gem532) is aimed upwards using a mirror and subsequently focused by a lens into a vacuum chamber (see figure 4). Furthermore, a rotating mount with a wave plate ($\lambda/2$ or $\lambda/4$), is placed above the lens, allowing for changes to be made to the laser polarization.

After exiting the chamber, the beam is vertically aligned using two apertures attached to a vertical pole at different heights. Ideally, the horizontal cross section of the beam is perfectly circular, with a Gaussian intensity distribution.

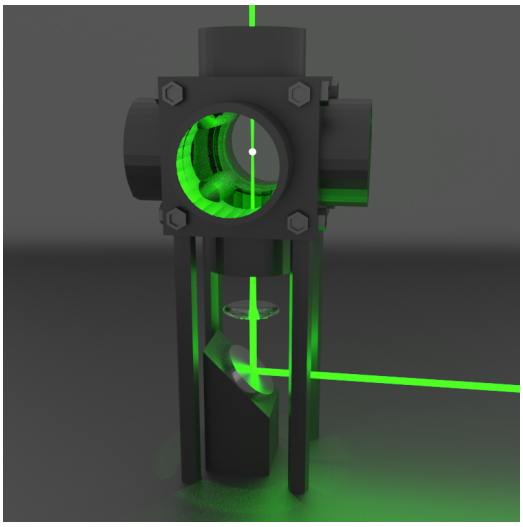

Figure 4: Simplified render of the experimental setup. A laserbeam hits a mirror, leading the beam into a lens which focuses the light at a point inside the vacuum chamber.

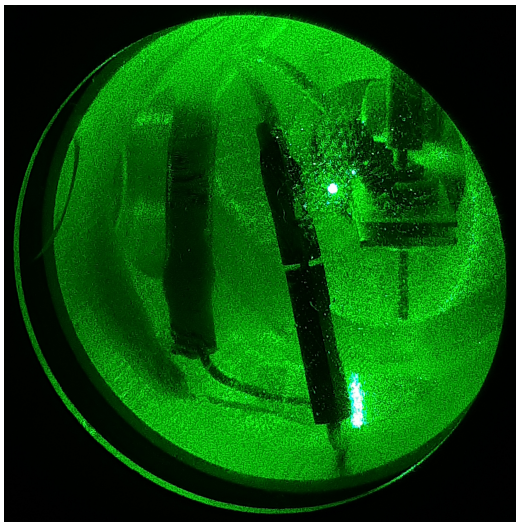

Figure 5: Close up picture of the chamber, with the centered light source being a levitating particle.

Perpendicular to the laser beam, a LED-light is pointed at the levitated particle, seen as a green light-spot in figure 5, and aimed towards a high speed camera placed at the other side of the chamber. The trapped particles block some of the LED-light, casting a shadow that is picked up by the camera. Footage from the camera is recorded and analysed using the open source software "Tracker: Video Analysis and Modeling Tool". Using this program, the position of recorded particles is extracted for further analysis.

3.2 Dispensing particles

A water solution containing spherical particles, with a specific diameter and standard deviation, is placed in a small droplet on a glass slide using a dropper. The droplet is subsequently heated, using a heat gun, until the liquid has evaporated, leaving a thin coating of particles stuck to the glass. The slide is placed over the laser beam and the optical trap is activated. The slide is then lightly tapped causing particles from the slide to detach and drop into the chamber. Several particles drop with each hit, most not aligned with the laser leading to them falling to the bottom of the chamber. But, some particles do align with the laser, which provides a decelerating force slowing their fall. If the amount of particles in free fall aligned with the laser is small, there is a chance that the decelerating force is enough to make a single particle levitate in thin air, thus trapping it. This process is illustrated in figure 6.

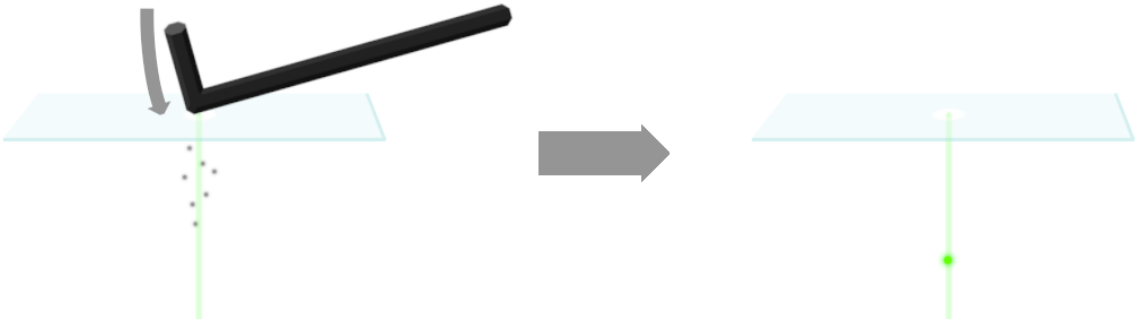

Figure 6: An illustration of the dispensing method. A slide holding on to a spot of particles is lightly tapped with a small tool. If a particle is released in alignment with the beam it may become trapped.

Two types of microspheres are used:

- Silica particles, diameter 24.82 µm ($\sigma = 1.06\,\mu\text{m}$), $\rho = 1.85\,\text{g}\,\text{cm}^{-3}$
- Polystyrene particles, diameter 24.80 µm ($\sigma = 0.55\,\mu\text{m}$), $\rho = 1.05\,\text{g}\,\text{cm}^{-3}$.

σ is the standard deviation of the diameter, while ρ is the density of the material. The method for dispensing particles does not significantly differ between the two.

A crust is sometimes formed, making the particles stick to slide when tapped. This problem has been noted to occur more frequently when using the polystyrene particles. By lightly tapping or scratching the surface of the dried particles with a small tool like a hex key, the crust is broken and the particles drop as intended.

3.3 Producing Dumbbells

Once a single particle has been trapped, it is possible to trap another particle using the same procedure. The particles released have a chance to collide with the already trapped particle, which can cause the particles to merge, creating a dumbbell. Dumbbells are heavier than single particles, thus requiring the beam power to be increased by approximately 50% for a dumbbell to be successfully trapped. A high power beam is also necessary to catch the newly formed dumbbell, which acquires a downwards facing momentum right after the two single particles collide. It is also possible to obtain a dumbbell by chance, if it detached from the plate already formed.

3.4 Changing the Polarization

As previously mentioned, the polarization of the beam could be changed in two ways. Firstly, the polarization could be changed from linear to circular by placing a quarter wave plate beneath the vacuum chamber, horizontally rotated 45° from the original direction of polarization. In order to test whether the rotation of the plate is correct, a linear polarizer is placed above the vacuum chamber, and the intensity of the light passing through is observed. If the light is indeed circularly polarized, the intensity will not change when the polarizer is rotated. In practice the polarization would always be slightly elliptical in some direction, as measurements were made manually, and it is thus impossible to ensure completely circular polarization.

Secondly, the direction of the polarization could be changed by placing a half wave plate beneath the chamber and rotating it to the desired direction. After rotating the plate 180°, the polarization will have rotated by 360°. In order to empirically determine the new direction, a polarizer could again be used to see in which direction the light is blocked.

3.5 Measurements

3.5.1 Motion

For observations of single particles, only its position is observed, but when observing dumbbells, the two spheres are tracked individually. By having data for the two spheres, the rotation and center of the dumbbell can be extracted with ease. To calibrate the scale of the data produced,

the distance between two electrodes, seen to the right of the trapped particle in fig 5, is measured to 0.8 mm. The shadow from these electrodes appear in the data as two rectangles, from which the 0.8 mm measurement can be used to calibrate the footage. From this calibration, a smallest distinguishable distance is calculated to approximately 1.9 µm by the software.

3.5.2 Trap stiffness

For the trap stiffness in the vertical direction, the motion of the particle is measured using a position sensitive device (PSD) which provides precise and high sample rate position data. By capturing a particle's motion, and applying a high-pass filter, the chaotic Brownian motion of a trapped particle is extracted. This data shows a particle's vertical displacement from its position of stability over time, and with this a histogram of the displacement-distribution is made. By multiplying the logarithm of the histogram with the Boltzmann factor ($-k_{\mathrm{B}}T$) the particles potential is obtained[9].

Once the potential is known, it is approximated with a polynomial of the second order which is then derivated to obtain the restoring force. With a leading coefficient a and a constant coefficient c, the factor $2a$ is equivalent with the trap stiffness, k, which can therefore be known,

$$U = ax^2 + c \implies F_{\mathrm{r}} = -2ax = -kx.$$

3.5.3 Effect of Linear Polarization

In order to measure how the dumbbells reacted to different directions of polarization, the half wave plate is placed in the rotating mount and manually rotated in intervals, while the dumbbell is recorded. Usually, the polarization direction would be rotated by an angle φ from 0° (corresponding to a polarization perpendicular to the viewing direction of the camera) to either 180° or 360°. The intervals are usually either 10° or 20°. At the beginning and end of every interval, the time is recorded. Every time an interval is completed, a few seconds are allowed to pass before beginning the next, to give the particle some time to stabilize. Thus, at the times between the intervals, when the angle is constant, φ is known exactly.

3.6 Simulation of Diffraction Patterns

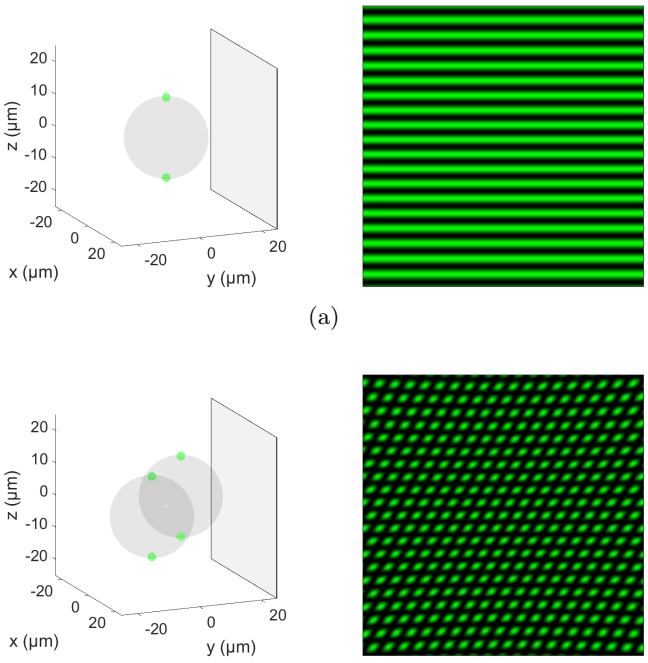

Figure 7: Point sources (left) and diffraction patterns (right) of a single particle and a dumbbell. The outlined plane shows the direction in which the diffraction patterns are simulated.

When the laser beam hits a single particle or a dumbbell, the light is scattered and results in diffraction patterns being produced in the far field. By simulating diffraction patterns and comparing the result with observations from the laboratory, the patterns can be used as a rule of thumb when determining dumbbell orientation. A simple method for simulating the diffraction patterns perpendicularly to the laser beam is to utilise the Huygens-Fresnel principle. Each particle is modeled using two spherical point sources, one on the bottom and one on top of the particle. In figure 7 the model is illustrated for both a single particle and a dumbbell.

Simulating diffraction patterns in line with the beam (i.e. vertical) requires another method. The wavefront of the laser beam is modeled as a two dimensional gaussian electric field, stored in a large matrix. A transmission function for an ideal lens is applied to the electric field. The transmission function is given by

$$T_{\text{lens}}(r) = \exp\left(-ikr^2/2f\right), \tag{17}$$

were k is the wave vector in air, r is the distance from the center of the lens and f is the focal length, 100 mm. It is then propagated using the angular spectrum method. Trapped particles are modeled as opaque spheres a short distance after the focal point of the lens (about 5 mm which is close to what has been observed in the laboratory). Once the electric field has been propagated to this point, the transmission function of the particles is applied and the electric field is propagated further, resulting in the patterns seen in figure 8.

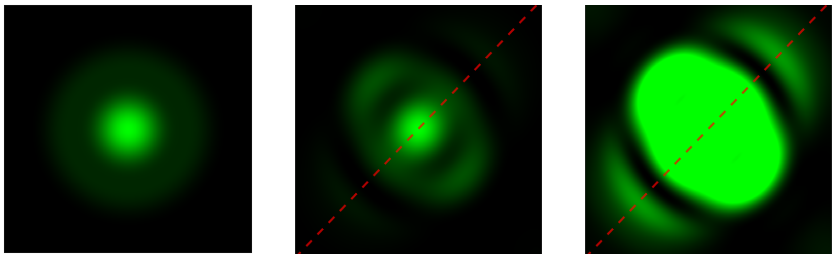

(a) (b) (c)

Figure 8: To the left (a), the vertical diffraction pattern of a single particle is illustrated. In the middle (b), the diffraction pattern depicted belongs to a dumbbell at an angle of 45° from the x-axis, indicated by a dashed red line. To the right (c), the saturation of the same pattern is increased, simulating what an overexposed camera would capture.

From the example simulation above, specifically figure 8c, it can be seen that the direction of the dumbbell tends to align with the dark lines closest to the center. However, due to overexposure, the diffraction pattern observed during experiments appeared to be rotated 90°. This phenomenon was reproduced by increasing the saturation of the simulated diffraction pattern.

4 Results

4.1 Single Particles

The long focal length resulted in a low trap stiffness in the vertical direction. This limited the movement of single particles to mainly one degree of freedom with barely any horizontal movement. The most common mode of motion was the stationary one, where the particle only moved slightly around a stable position. Alternatively, particles would often display a crawling motion where the particle first descends slowly, followed by a quick ascension.

As previously mentioned, when a particle is trapped, it blocks out some of the light from the laser and acts as a sort of aperture, giving rise to diffraction patterns. These patterns become visible when hitting a surface. In figure 9, the patterns produced by a trapped microparticle are exemplified and compared with the corresponding simulation. Depending on whether the diffraction patterns are viewed from the side, producing what can be termed horizontal diffraction patterns, or whether they are viewed above the trapped particle, producing vertical diffraction patterns, the patterns take on a different form. The comparison below is mostly congruent, except for what is likely spherical aberrations produced by the trapping lens.

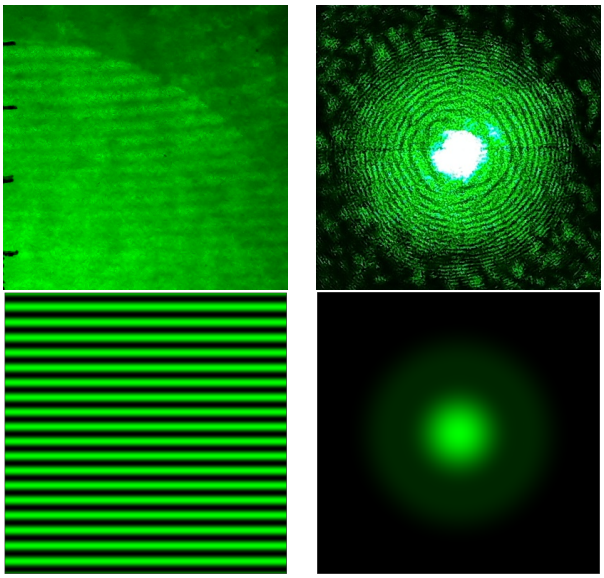

(a) (b)

Figure 9: An example of the diffraction patterns from one trapped particle compared to corresponding simulations. To the left (a) is the pattern as seen from the side, perpendicularly to the trapping laser beam. To the right (b) is the diffraction pattern as seen above the optical trap.

4.1.1 Trap Stiffness

The vertical potential well for a trapped single particle can be seen in figure 10. A polynomial of the second degree is fitted to this potential (using 15 data points closest to the center of the potential) and with this the trap stiffness is found to be $k_{\text{single}} = 40.6 \pm 2.9$ nN/m.

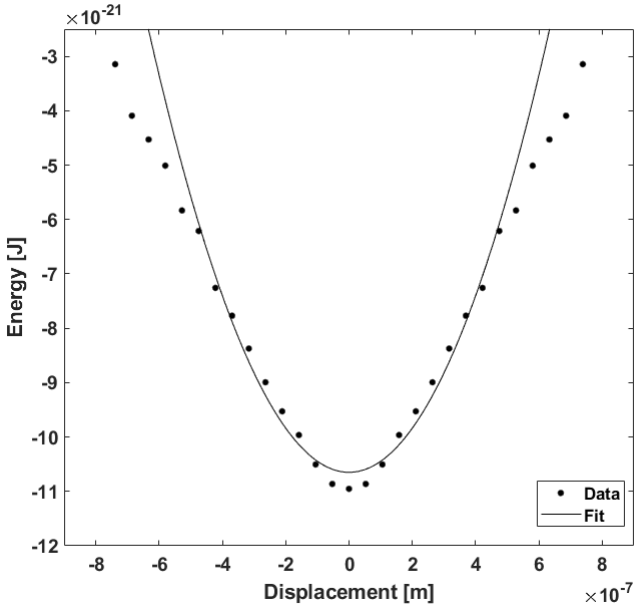

Figure 10: Potential of a single polystyrene particle.

4.2 Dumbbells

Two types of dumbbells were observed, dancing and tilting, both illustrated in figure 11. Tilting dumbbells, those produced by merging two particles as described in section 3.3, stayed mostly still except for vertical movements induced by fluctuations in the laser and their dependence on polarization. Dancing dumbbells, often those that dropped from the slide as fully formed dumbbells, exhibited a rapid oscillatory motion when trapped.

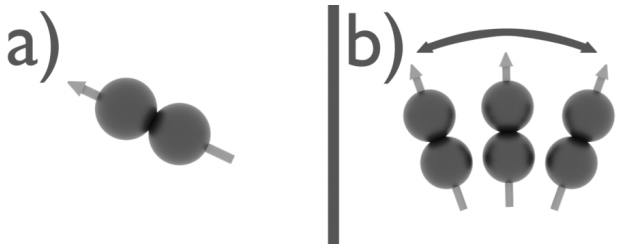

Figure 11: An illustration comparing tilting and dancing dumbbells. a) A tilting dumbbell, resting at a stable angle. b) A dancing dumbbell, shown at multiple times during its dance back and forth.

The rotating plane, illustrated as the xz-plane in figure 12, is defined as the plane spanned by the dumbbells long axis, defined as the line which intersects with the centers of both particles, and the vertical axis.

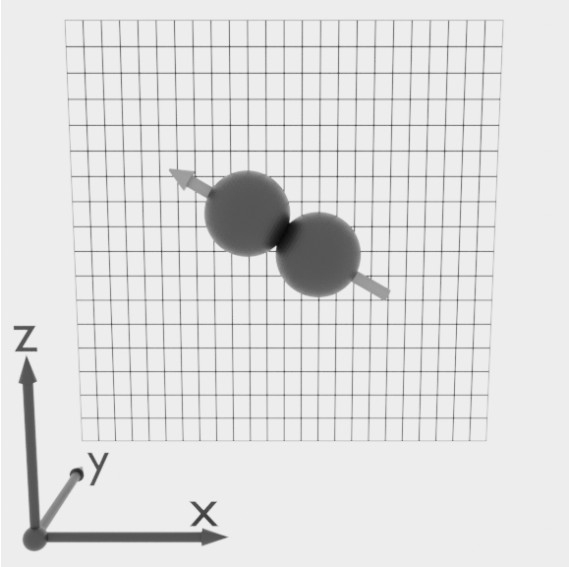

Figure 12: An illustration of the rotating plane, seen as the xz-plane in which the dumbbell exists.

The different kinds of dumbbells would exhibit different angles to the horizontal plane when trapped. Dancing dumbbells would have their longer axis oscillate around a vertical position, thus being regarded as standing up in the trap. The tilted dumbbells would, at rest, have a horizontal angle in the range $20° - 50°$. These tilted dumbbells would sometimes do a turnover, thus effectively rotating 180° around the vertical axis and "flip" in its rotating plane, see figure 13. Whether this was due to a rotation around the vertical axis, or a rotation in the plane, was often difficult to determine.

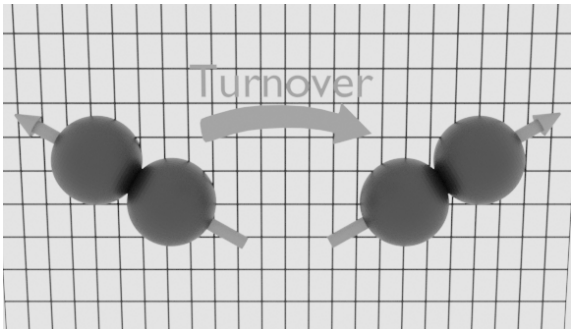

Figure 13: Illustration of a dumbbell turnover, notice that it stays in its rotating plane.

4.2.1 Trap Stiffness

The potential for a trapped dumbbell can be seen in figure 14. A polynomial of the second degree is fitted to this potential (using 15 data points closest to the center of the potential) and with this the trap stiffness is found to be $k_{\text{dumb}} = 35.88 \pm 1.12$ nN/m.

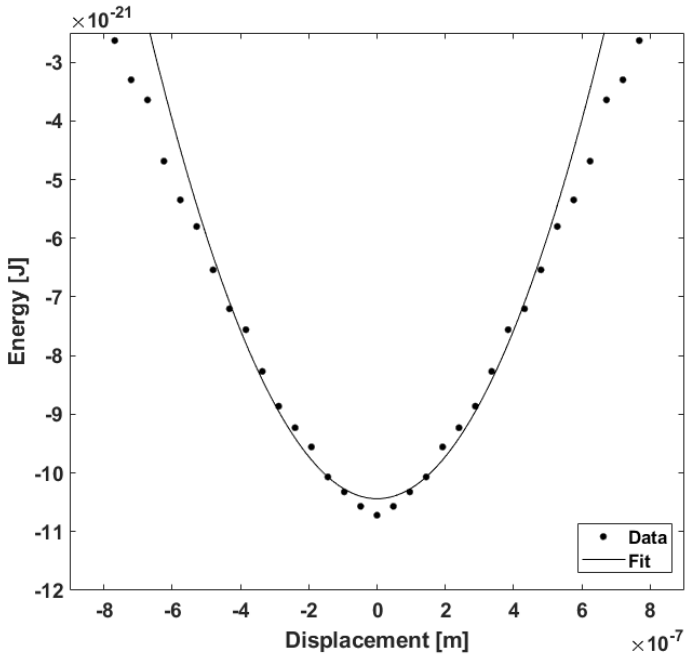

Figure 14: Potential of a polystyrene dumbbell.

The polynomial approximations of the single particle potential, see figure 10, and dumbbell potential are presented in figure 15.

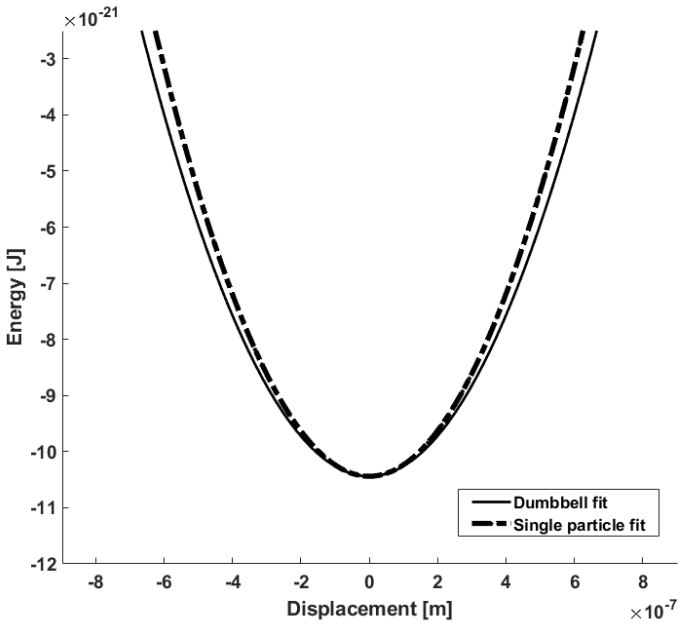

Figure 15: The fitted single particle potential, see the dashed line, compared to the fitted dumbbell potential.

4.3 Effects of Polarization

The effect that polarization had on a dumbbell would vary depending on its elevation in the trap, thus being dependant on the lasers intensity which is correlated with the elevation by equation 9. Two broad regimes can be identified depending on elevation, the rotating and the stationary regime. In figure 16, these regimes are illustrated, the lowest of the dumbbells representing the rotating regime, and the two upper dumbbells representing the stationary regime.

In the rotating regime, the rotating plane of a tilting dumbbell would be perpendicular to the polarization and stay this way as the polarization is rotated. For a dancing dumbbell, the rotating plane would instead be parallel with the polarization.

At higher elevations where the stationary regime ensues, the tilting dumbbell remains suspended in a given direction, seemingly correlated with its elevation. The effect of changing polarization at this level is weak. Around its preferred direction, the dumbbell would often display small wiggles at a magnitude of about 10°. This effect was observed when the polarization was roughly perpendicular to the direction of the dumbbell. Dancing dumbbells have not been investigated in this regime.

Between the rotating regime and the stationary regime, an intermediary state can be observed. In this state, the dumbbell rotates quite freely while showing a clear preference for certain directions. Sometimes, the dumbbell would stop either completely or only momentarily. In the case of a short stop, a turnover would sometimes be induced.

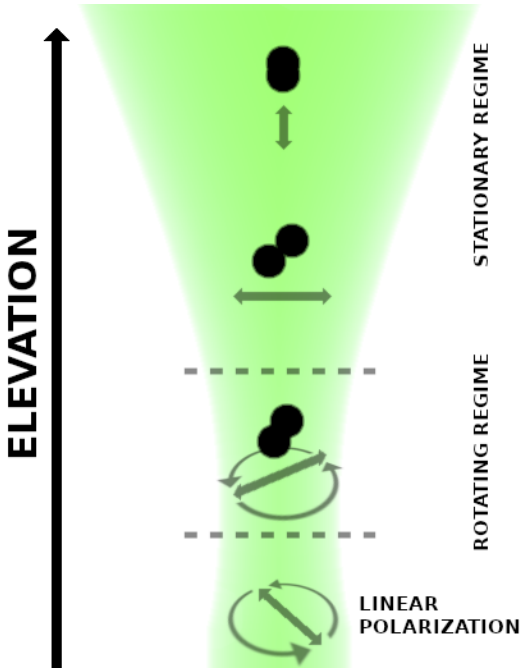

Figure 16: An illustration of the different regimes observed in tilting dumbbells when subject to rotating linear polarization. At lower elevations, in the rotating regime, the dumbbell follows the polarization at a 90° angle. At higher elevations, in the stationary regime, the dumbbell remains suspended in a direction that varies according to its elevation or the intensity of the laser. This image is not to scale.

Circular polarization was not observed to create any particular alignment except in the case where the polarization was not entirely circular. This polarization should be regarded as elliptic and had a similar effect to linear polarization, with the dumbbell lining up along the elongated axis of polarization.

4.3.1 Tilting dumbbells

One case in the rotating regime, in which the direction was roughly perpendicular to the polarization, is presented qualitatively in figure 17. This figure shows some images captured by the camera for different values of φ, the angle denoting how much the polarization had been rotated from the original position where it was perpendicular to the camera direction. The change in tilt direction between 40° and 90° is due to an instantaneous dumbbell turnover which occurred at 80°. It is also possible that a turnover happened at 180°, although this is difficult to determine.

The particles were composed of polystyrene.

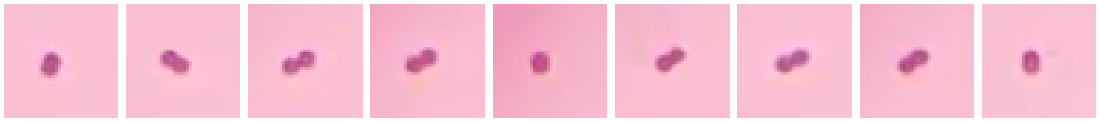

Figure 17: A selection of images captured by the camera. The angle beneath each image denotes φ, the angle by which the polarization had been rotated. Note that at 0° the polarization is parallel to the image, and the particle thus levitates perpendicularly to the polarization. It can be seen qualitatively that the horizontal distance between the polystyrene particles varies in sync with φ. Between 40° and 90° the dumbbell performed a quick turnover, effectively flipping around the vertical axis. This may also have occurred at 180°.

This case can also be studied quantitatively in figure 18. At the beginning, with the polarization perpendicular to the camera, the rotating plane was roughly parallel to the direction of the camera, resulting in a small mean distance between the two particles. The distance was calculated as the apparent horizontal distance between the centre points of the two particles as seen from the camera in figure 17. As the polarization angle, φ rotated in intervals of 20°, the mean distance increased, and reached a maximum at around 90° and 270°, before decreasing to a minimum at 180° and 360° respectively. Thus, these results indicate that the rotating plane was always perpendicular to the polarization. Whether the plane also rotated 360°, or if it only rotated some multiple of 90°, before switching direction, can not be seen from this data, as the camera only sees a 2D projection of the dumbbell.

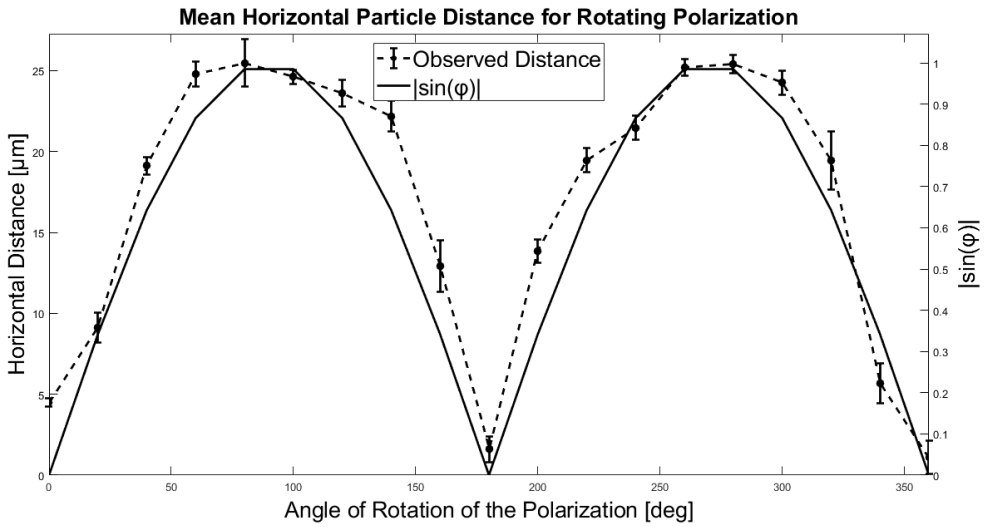

Figure 18: Effect of rotating the laser's polarization on the orientation of the polystyrene dumbbell. In this instance, in the rotating regime, the polarization was rotated 360° in intervals of 20°, from an original position perpendicular to the camera direction. The horizontal axis is the rotation angle φ. The dots on the dashed line indicate the mean horizontal distance at the 19 rotation angles where φ was temporarily constant. The error bars correspond to one standard deviation in each direction. The solid line indicates the value of $|\sin(\varphi)|$ at those angles.

A similar case is presented in figure 19. This was also in the rotating regime, with polystyrene particles. Here, φ goes up to 180° in intervals of 20°, but the big difference as compared to the previous case, is that the rotating plane is not quite perpendicular, although still rotating roughly in sync with the polarization. Instead, it seems to be offset by about 20° at the start, as it only becomes parallel with the camera, resulting in a minimal distance, once the polarization has rotated by $\varphi \approx 20°$. As φ increases, the phase shift seems to decrease. This behaviour was often observed,

although it was most common for the plane to be perpendicular to the polarization.

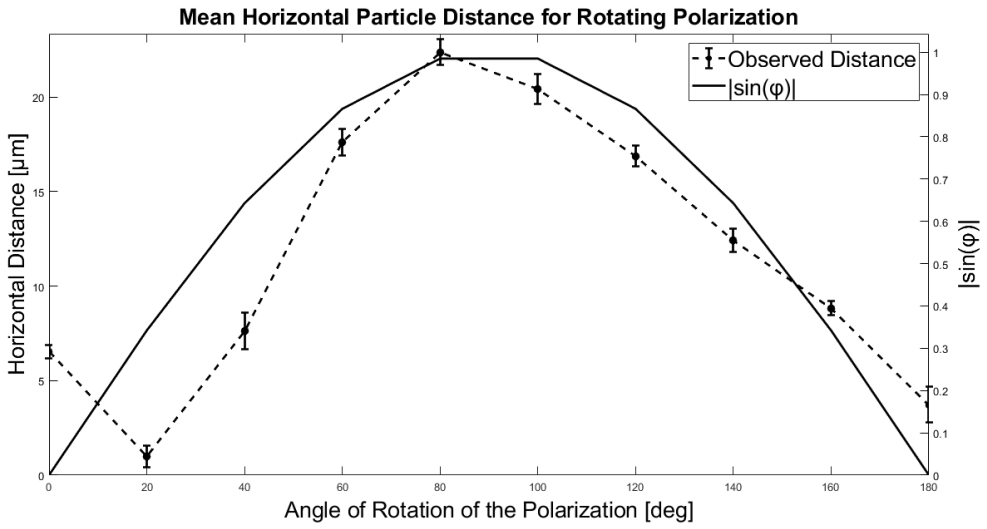

Figure 19: Effect of rotating the laser's polarization on the orientation of the polystyrene dumbbell. The dots on the dashed line indicate the mean horizontal distance at the 10 rotation angles where φ was temporarily constant. The solid line indicates the value of $|\sin(\varphi)|$.

A similar result to what is seen in figure 19 can also be seen when studying the diffraction patterns in figures 20 and 21. In the first panel the vertical diffraction pattern is shown to follow the polarization angle, once again shifted by about 20°. However, due to overexposure, the simulation does not look like the diffraction patterns until this has been taken into account.

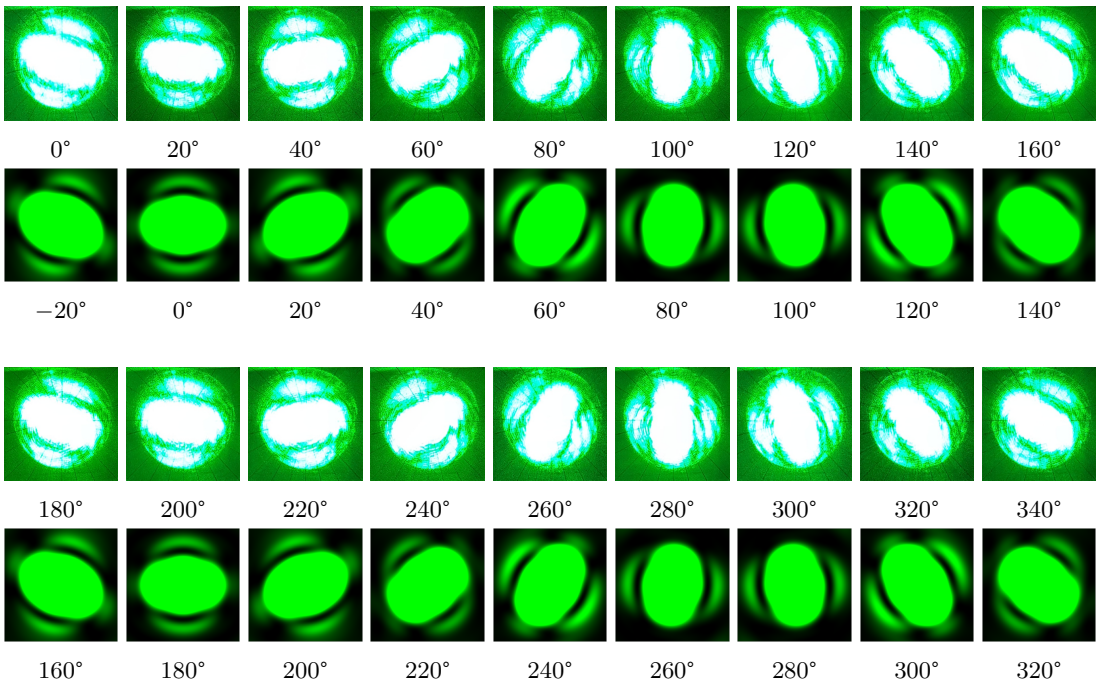

Figure 20: The vertical diffraction patterns (above) line up with the patterns produced by a simulation (below), shifted about 20° with regards to the direction of polarization.

The horizontal diffraction patterns corroborate the observations above. In figure 21, the first three images from a longer series show the same phase shift of about 20°.

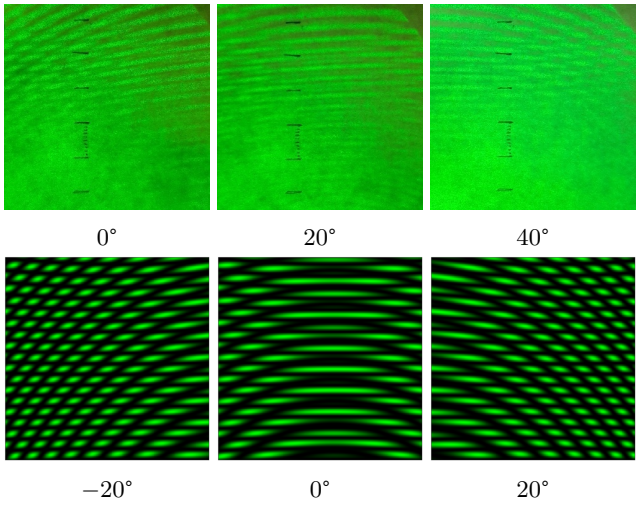

Figure 21: The first three horizontal diffraction patterns in a series line up with the patterns produced by a simple simulation, although shifted about 20° relative to the direction of polarization.

In figure 22, the horizontal center of mass of a dumbbell in the rotating regime is shown to vary depending on the angle of polarization. The difference between the maximum and minimum position is about 15 µm.

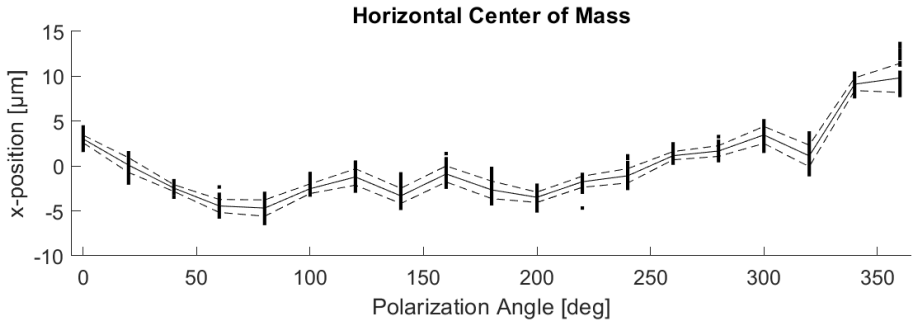

Figure 22: The horizontal center of mass of a tilting dumbbell within the rotating regime changes according to the polarization angle.

In figure 23 the rotation and tilt of a dumbbell in the stationary regime is illustrated. The rotation was seen to follow the polarization angle within a narrow interval. Interestingly, the tilt shows a clear dependence on the polarization as well.

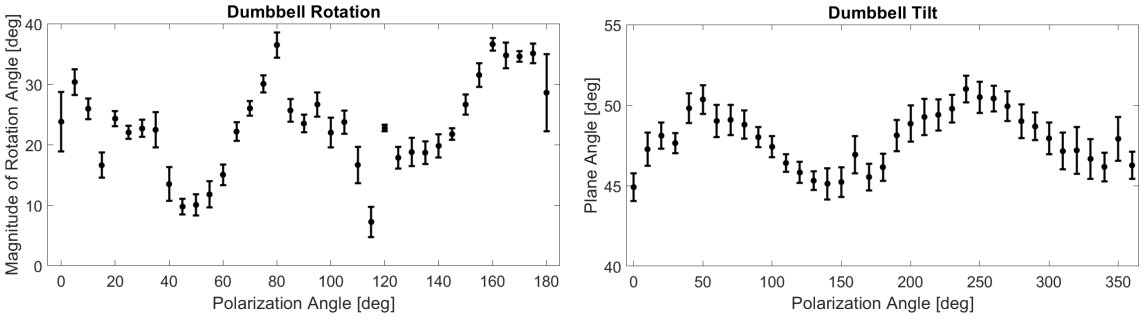

(a) (b)

Figure 23: Under changing polarization angle, a dumbbell trapped at high laser power remains relatively unchanged in terms of rotation (a) and tilt (b) when subject to different polarization angles.

4.3.2 Dancing dumbbells

The oscillation amplitude of dancing dumbbells as the angle of linear polarization changes is illustrated in figure 24. The amplitude shows a sinusoidal dependence on the angle, albeit somewhat shifted in phase. In the same figure, the mean center of mass stays close to constant.

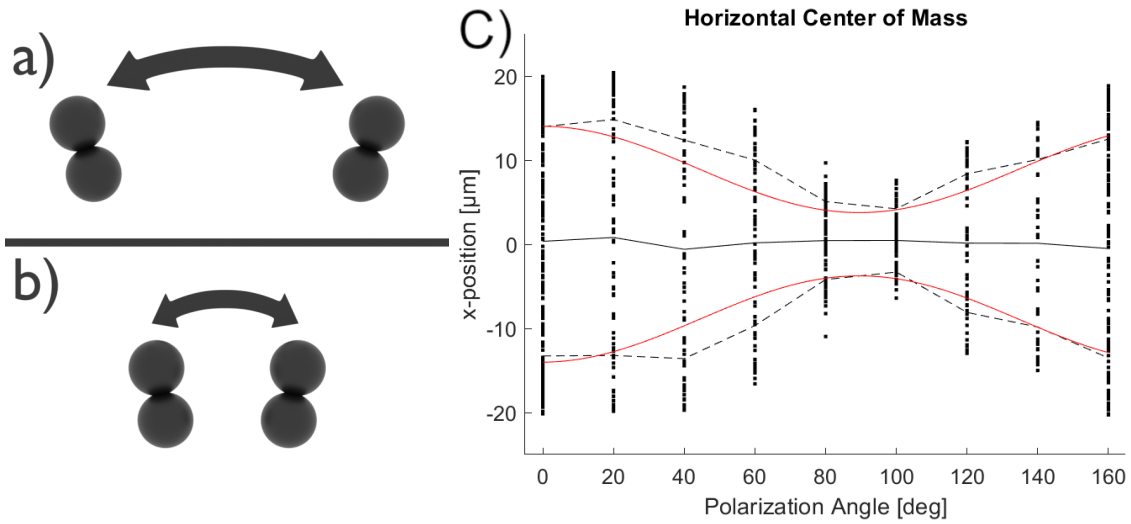

Figure 24: An illustration of the maximum amplitude of dancing particle and the horizontal center of mass of one of these particles. a) A dancing dumbbell dancing with a large amplitude, as the polarization is perpendicular to the observer. b) A dancing dumbbell with less amplitude as the polarization is not perpendicular to the observer. c) The mean horizontal center of mass for a dancing dumbbell, represented by the solid line black line in the middle, is calculated from the individual data points, plotted in vertical lines. The dashed lines represent the standard deviation of the same and illustrate that the amplitude of the oscillation varies with respect to the polarization angle. Lastly, the solid red lines roughly aligned with the dashed lines represent expected values.

4.4 Oscillatory and Periodic Motion

Silica dumbbells trapped in circularly/elliptically polarised light would sometimes exhibit a complex periodic oscillatory behavior. Depending on the y-coordinate of the center of mass of the dumbbells, the amplitude of the oscillation would vary. In figure 25a and 25b measurements are plotted in a phase space diagram where the horizontal axis corresponds to the y-position of the dumbbell center of mass, and the vertical to the amplitude of the oscillation. The frequency of the oscillation when trapped in a circularly polarised, 532 nm wavelength laser beam, was constant at about 35 ± 1.1 Hz.

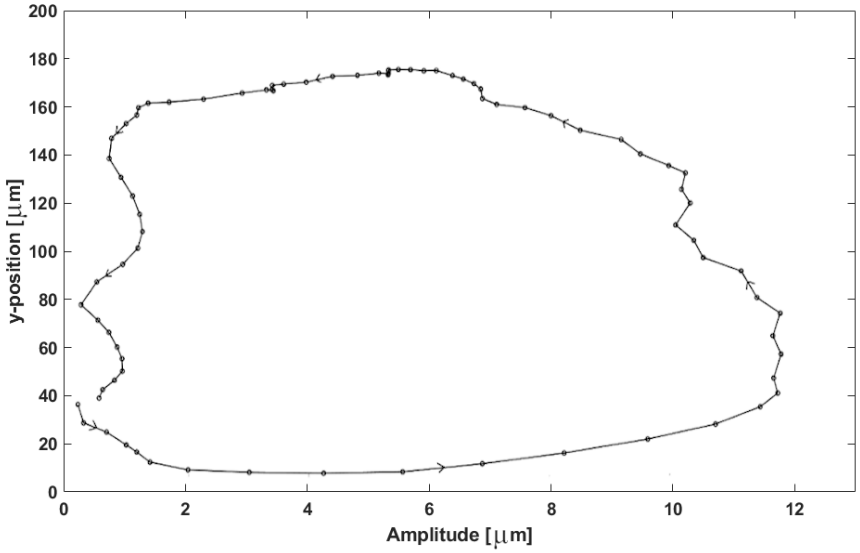

(a) Hysteresis is clearly shown as the dumbbell gain oscillation amplitude, begins to rise, decreases in amplitude and falls.

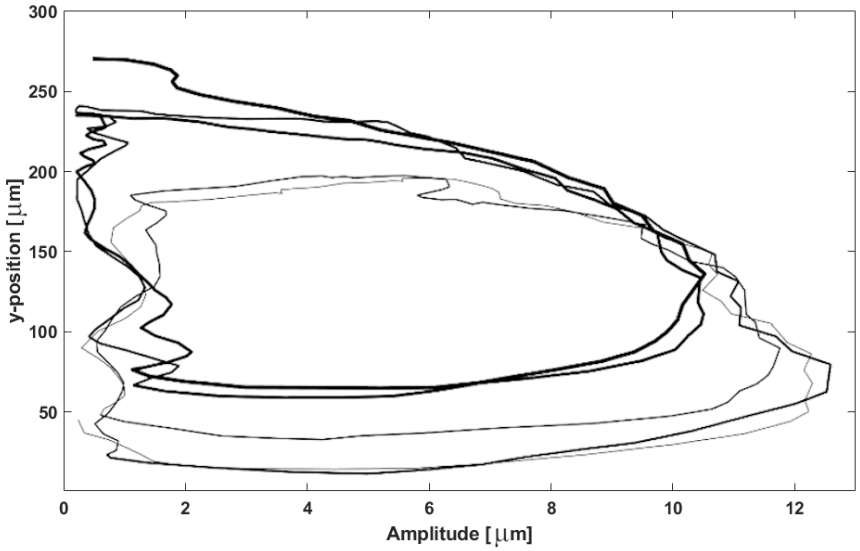

(b) The same behavior as figure 25a with several intervals, each illustrated with a different thickness to separate them.

Figure 25: A hysteresis pattern repeats as the dumbbell experience circular/elliptical polarization.

As the oscillations take place, the mean angle of the dumbbells long axis to the horizontal plane changes. This mean angle for some of the periods shown in figure 25b can be seen in figure 26, which shows a clear connection between the mean angle and vertical position. The start in rise of mean angle, see the lowest point between the black bars in figure 26, takes place at the same time as the particle starts to oscillate.

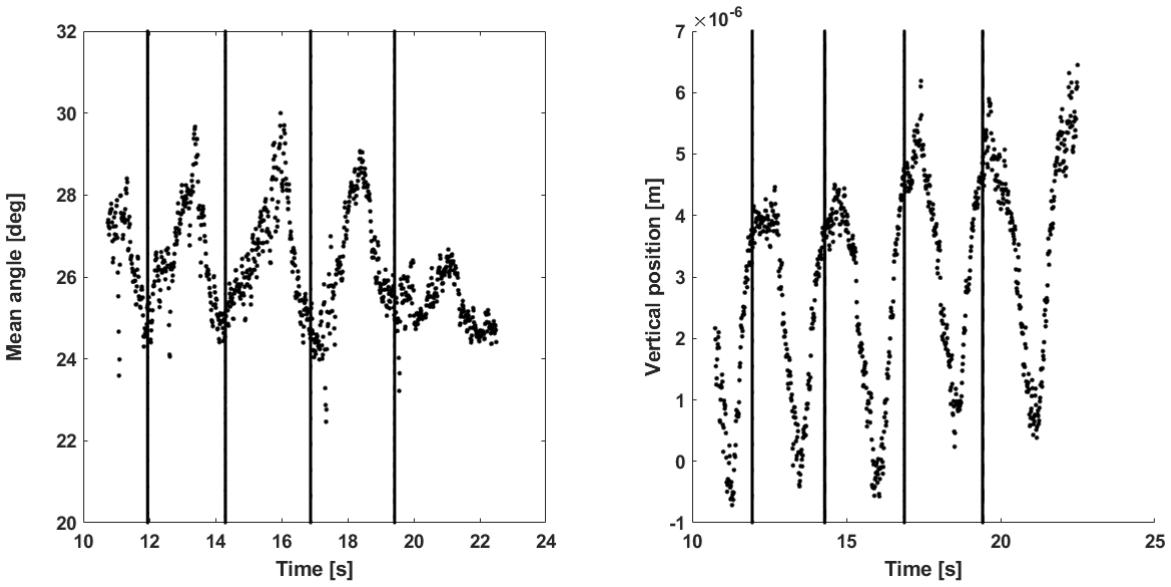

Figure 26: Left: The change in average angle during the periodic oscillatory motion. The vertical lines are the points where the dumbbells reach their upper y-position in every period, which is in sync with the minimum mean angle. Note that at the minimum points between the black line is the start of the new oscillations. Right: The vertical position of the dumbbell with the same black lines as in the left figure.

5 Discussion

5.1 Comparison of Trap Stiffness

Comparing the trap stiffness of a dumbbell to that of a single particle, the following is found,

$$\frac{k_{\text{dumb}}}{k_{\text{single}}} = 0.890 \pm 0.091, \tag{18}$$

which indicates that the trap stiffness for a dumbbell is less then that of a single particle. The dumbbell has a bigger cross-sectional area than the single particle. A dumbbell at zero degrees, that is laying horizontal, would have twice the cross-section of a single particle thus being affected by twice the scattering force.

A dumbbell at the angle γ from the horizontal plane would have an approximated horizontal cross-section of,

$$A_{\text{hor}} = (1 + \cos\gamma) \cdot A_{\text{single}}, \tag{19}$$

where A_{single} is the single particles cross-section.

Since the scattering force is proportional to the horizontal cross-section, the force applied to dumbbells would be larger than that applied to a single particle (according to eq. 19). We propose that the force that these particles feel is proportional to their cross-sectional area and that the harmonic potential depends inversely proportional to mass, leading to the following,

$$F_{\text{single}} = \alpha \cdot \frac{A_{\text{single}}}{m}, \ \alpha = \text{constant of proportionality}, \tag{20}$$

$$F_{\text{dumb}} = \alpha \cdot \frac{A_{\text{hor}}}{2m} = \alpha \cdot \frac{(1 + \cos\gamma)}{2m} \cdot A_{\text{single}}, \tag{21}$$

$$\implies \frac{F_{\text{dumb}}}{F_{\text{single}}} = \frac{(1 + \cos\gamma)}{2}, \tag{22}$$

meaning we should see a bigger restoring force on a trapped single particle for $\gamma > 0$.

From this model the relative trap stiffness would be derived from,

$$\frac{k_{\text{dumb}} \cdot x_{\text{dumb}}}{k_{\text{single}} \cdot x_{\text{single}}} = \frac{F_{\text{dumb}}}{F_{\text{single}}} = \frac{(1 + \cos\gamma)}{2}. \tag{23}$$

By displacing both particles the same length, $x_{\text{single}} = x_{\text{double}} = x$, one obtains,

$$\frac{k_{\text{dumb}}}{k_{\text{single}}} = \frac{F_{\text{dumb}}}{F_{\text{single}}} = \frac{(1 + \cos\gamma)}{2}. \tag{24}$$

Entering some common angle $\gamma = 30°$ that we usually see, the following is found,

$$\frac{k_{\text{dumb}}}{k_{\text{single}}} = \frac{(1 + \cos 30°)}{2} = 0.933 \tag{25}$$

which falls within the measured value from eq. 18. Therefore, this might be a good model for trap stiffness dependence on geometry.

5.2 Effects of Polarization

Both tilting and dancing dumbbells seem to be affected by polarization in one regime, the rotating regime, where its elevation is relatively low at a distance of around 105 mm from the trapping lens. Tilting dumbbells follow the polarization perpendicularly while dancing dumbbells align with the polarization. The results seem to be inconclusive in regards to explaining these phenomena but they do provide some clues.

Firstly, In figure 22, a shift of horizontal center position of about 15 µm is seen. Using the data sheet of Laser Quantum gem 532 [10], an approximation of the beam waist can be made. The beam diameter, as given in the data sheet is approximately 1 mm. Using equation 12, the

diameter of the beam at the focal length is approximated to 68 µm. The horizontal shift of about 15 µm may thus be significant. If tilting dumbbells follow the polarization as a result of a sort of force imbalance caused by its off centered position, then that may explain why this effect ceases at higher elevation, in the stationary regime. Using equation 11 to calculate the Rayleigh length, we get about 6.8 mm, meaning that the beam diameter may increase by as much as 40 % within this distance. Since the rotating regime is already close to 5 mm past the focal length, the beam profile should be much bigger than the dumbbell in the stationary regime. However, this does not seem to explain why dancing dumbbells align differently.

Light approaching a surface will be reflected more if the direction of polarization is perpendicular to the plane of incidence. A possible explanation could thus be that the gradient force on a particle is stronger if the displacement from the center occurs parallel to the polarization, and weaker if the displacement is perpendicular. This could mean that it is energetically preferable for the dumbbell to align perpendicularly to the polarization.

Furthermore, in the rotating regime, dumbbells often show a small angular offset as is seen in the diffraction patterns and corresponding simulated patterns in figure 20. This type of behavior was often seen when weening close to the stationary regime, implying that it could be a transitional stage. Another possibility is that a systematic error in the polarization angle was present during some measurements.

In the stationary regime, tilting dumbbells are not completely stationary. As is illustrated in figure 16, as the laser power (corresponding to elevation) was increased, the stationary state of the dumbbell would rotate. It is not known whether it was the elevation or the laser power that was the root cause of this effect. It is interesting to note that the even the tilt seems to vary according to polarization, something which could potentially be tied to oscillatory behavior under circular polarization.

5.3 Oscillatory and Periodic Motion in Dumbbells

When elliptical polarization was used to levitate silica dumbbells, they were in some cases found to oscillate, illustrated in figure 27a. When the amplitude of this oscillation increased, the dumbbell started to rise upwards in the trap. As it rises, the amplitude of oscillation would decrease and when completely still, it would fall to a lower vertical position. This cycle can be seen in figure 27.

One explanation is that the oscillation is an effect of the elliptical polarization, which rotates the lasers electric field and changes the dumbbells stability position. When affected by a constantly changing point of stability, the dumbbell might become a damped driven harmonic oscillator, thus oscillating.

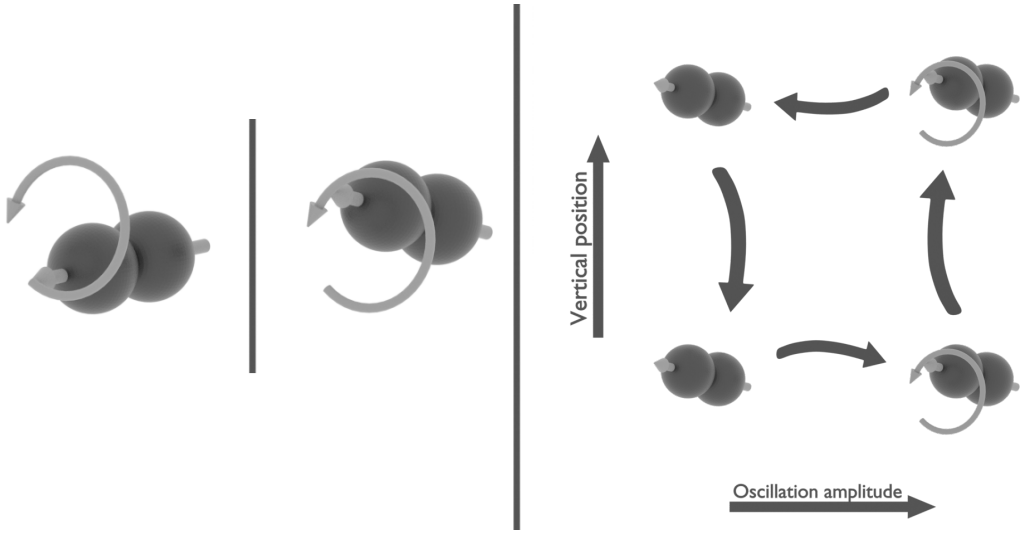

(a) (b)

Figure 27: Illustration of the oscillatory motion of dumbbells. a) Dumbbell oscillation, shown as two dumbbells at different points in their oscillation, with oscillation amplitude depicted as a bent arrow. b) One full period of the complex oscillatory behavior. The arrows in the figure represent the order of events.

As seen in figure 26, the mean angle of the dumbbell changes when its oscillation amplitude increases, reaching its minimum value right before the oscillations stop. This might change the dumbbells horizontal cross-section, which reaches its maximum when the absolute value of the mean angle is at its lowest point. A bigger horizontal cross-section implies a larger area for the lasers scattering force, which would lead to an increasing vertical position in the trap.

When studying linear polarization, depending on how far the levitated particle is from the focal length of the trapping lens it would react differently to the polarization. Close to this point, the particles would follow the polarization as it rotates, but at higher positions the particles did not follow the polarization as well. This might be an explanation for the diminishing oscillation amplitude of the dumbbell as it rises, because as it rises it feels less of the polarization and comes to a stop. At this point, the mean angle has decreased (observe the mean angle after each black line in figure 26) as the oscillation amplitude disappears. This leads to a decline in the horizontal cross-section, which probably reduces the scattering force on the dumbbell, thus lowering its position.

As the vertical position declines, the dumbbell would once again fall close to the focus point, and therefore feel the effect of the polarization once again and start to oscillate. This creates a cycle which repeats according to figure 25b, the cycle is also illustrated in 27b.

6 Conclusions and Outlook

6.1 Regimes

It is clear from the data that tilting dumbbells within a slim regime close to the focal length of the trapping lens follow the polarization perpendicularly. Dancing dumbbells in the same regime align in parallel with the polarization. When rising above this regime, dumbbells would reach a point where they no longer experience the effect of a change in polarization. This is a deviation from what has been reported for dumbbells (and similar oblong objects) at nanoscale, indicating a clear dependence on size and/or mass. Research with dumbbells smaller than the ones used in this thesis could prove helpful for understanding how scale changes the dynamics of oblong levitated objects. This could be done by investigating different dumbbells with varying volume and density, and particularly observing how they react to polarization.

6.2 Oscillatory motion

The complex oscillatory cyclic motion of the dumbbell is believed to be caused by moving between the different regimes where the polarization's effect varies. Future research focused on mapping out the dumbbells dependence on polarization due to height might give insight about the oscillatory motion. Additionally, the dumbbell always aligned the same direction when under circular polarization, this is believed to either be due to an elongated beam cross-section or that the polarization was more elliptical than circular. So, dumbbell levitation experiments using elongated beam cross-sections and elliptical polarization in different directions might give some information regarding why dumbbells in circular polarization aligns a certain way.

6.3 Turnover

Turnovers, illustrated in figure 13, would sometimes occur when observing dumbbells. Although no strong pattern of when this would happen was recorded, they usually exhibited this behavior during rotation of polarization. Additionally, little data was gathered regarding the dynamics of a turnover. If a way to precisely induce turnovers is discovered, their behavior could be further studied. One hypothesis is that the turnover takes place between positions of stability. Therefore, it would be interesting to see if there is a link between *Kramers turnover* [11] and the dumbbell turnover rate under different levels of air pressure.

References

[1] A. Ashkin, "History of optical trapping and manipulation of small-neutral particle, atoms, and molecules," *IEEE Journal of Selected Topics in Quantum Electronics*, vol. 6, no. 6, pp. 841–856, 2000.

[2] J. Bang, T. Seberson, P. Ju, J. Ahn, Z. Xu, X. Gao, F. Robicheaux, and T. Li, "Five-dimensional cooling and nonlinear dynamics of an optically levitated nanodumbbell," *Physical Review Research*, vol. 2, Oct 2020.

[3] J. Ahn, Z. Xu, J. Bang, Y.-H. Deng, T. M. Hoang, Q. Han, R.-M. Ma, and T. Li, "Optically levitated nanodumbbell torsion balance and ghz nanomechanical rotor," *Physical Review Letters*, vol. 121, Jul 2018.

[4] S. Kuhn, A. Kosloff, B. A. Stickler, F. Patolsky, K. Hornberger, M. Arndt, and J. Millen, "Full rotational control of levitated silicon nanorods," *Optica*, vol. 4, p. 356, Mar 2017.

[5] A. Ashkin, "Optical trapping and manipulation of neutral particles using lasers," *Proceedings of the National Academy of Sciences*, vol. 94, no. 10, pp. 4853–4860, 1997.

[6] J. T. Marmolejo, *Optical levitation of droplets, Whispering gallery modes, harmonic resonance and charge quantization.* PhD thesis, National Autonomous University of Mexico, 2019.

[7] A. Ashkin, "Forces of a single-beam gradient laser trap on a dielectric sphere in the ray optics regime," *Biophysical Journal*, vol. 61, no. 2, pp. 569–582, 1992.

[8] S. A. Self, "Focusing of spherical gaussian beams," *Appl. Opt.*, vol. 22, pp. 658–661, Mar 1983.

[9] J. T. Marmolejo, M. Urquiza-González, O. Isaksson, A. Johansson, R. Méndez-Fragoso, and D. Hanstorp, "Supplementary information, visualizing the electron's quantization with a ruler," *Sci Rep*, vol. 11, no. 10703, 2021.

[10] Laser Quantum, Stockport, UK, *gem High specification OEM CW lasers.* [Online]. Available: https://www.laserquantum.com/download-ds.cfm?id=1102, Accessed on: 2021-05-14.

[11] L. Rondin, J. Gieseler, F. Ricci, R. Quidant, C. Dellago, and L. Novotny, "Direct measurement of kramers turnover with a levitated nanoparticle," *Nature Nanotechnology*, vol. 12, pp. 1130–1133, Oct. 2017.